Green Kenaf-Based Adsorbent for Adsorption of Pb (II) Ions in Water

N. A. S. Anuar, S. Abdul-Talib, T. Chia-Chay, S. Abdullah, J. Jaafar, and N. F. Lokman

***Abstract*—Excessive toxic metals are commonly found in polluted water bodies. This study aimed to synthesise kenaf-based adsorbents for the adsorption of lead (II) ions. The physical and chemical characteristics of the kenaf (KNF) core and fibre were determined using field emission scanning electron microscope (FESEM), thermogravimetric analysis (TGA), and Fourier-transform infrared spectroscopy (FTIR). The further synthesised kenaf-chitosan-alginate (KNF-CHT-ALG) beads were characterised through FESEM and FTIR, while inductively coupled plasma (ICP) was employed to determine the percentage of adsorption. The FESEM analysis demonstrated that the KNF core had a rougher surface morphology than the KNF fibre. The TGA analysis confirmed that the KNF core was coarser and contained a higher residue of approximately 75.91%. The FTIR spectra established intense functional groups in the KNF core, such as hydroxyl and carboxyl, attracting more Pb (II) ions. The KNF core was then used to synthesise KNF-CHT-ALG beads. The beads confirmed the enhancement in surface morphology and the existence of numerous functional groups for Pb (II) ions to bind. The ICP analysis demonstrated 95% of Pb (II) ion adsorption. Additionally, batch adsorption experiments were conducted at pH 2–7 and the contact time was within 5–60 minutes. The kinetic study of the adsorption followed the pseudo-second order model with an R^2 value of 0.9999. The KNF is a crop found in abundance in Malaysia, which could reduce the production cost of adsorbents. The significant outcomes would minimise the dependency on chemical adsorbents and accelerate the removal process of heavy metals in natural bodies of water.**

***Index Terms*—Toxic metals, kenaf, polluted, adsorbent, adsorption.**

I. Introduction

Heavy metals are toxic and non-biodegradable constituents commonly found in various aquatic environments. Heavy metals are naturally low in aquatic ecosystems but could increase due to natural or anthropogenic sources that penetrate the water body and harm aquatic lives. Moreover, untreated heavy metals from various industries, including mining, electroplating, automotive, battery enterprises, and agricultural activities, have resulted in wastewater contamination [1]. For instance, the maximum lead (II) (Pb (II)) ions concentration in the Langat River Basin, Malaysia, was 9.99 ± 1.40 μg/L [2], which exceeded the permissible limit by the Department of Environment (DOE) Malaysia.

Ion exchange, membrane filtration, and chemical precipitation could be applied to treat heavy metals toxicity. Nevertheless, these methods are considered expensive and ineffective. The advantages of the adsorption method include low capital and operational costs, high performance, ease of operation, variation in adsorbent availability, and not being easily affected by harmful toxic substances [3]-[5]. Recently, adsorption methods that employ green adsorbent materials, such as chitosan (CHT) and kenaf (KNF) have been gaining attention due to their strong adsorption properties [6].

The CHT was extensively considered for its capability to absorb various heavy metal ions due to its functional groups, such as the amino ($-NH_2$) and hydroxyl (-OH) radicals [7]. Furthermore, a previous study used sodium alginate (ALG) as the cross-linking agent that enhanced the hydrophobicity of chitosan [8]. An abundant local plant known as KNF is another potential adsorbent with several functional groups that could enhance the stability of heavy metals adsorption [9], [10]. The adsorption mechanism of metal ions are demonstrated by equations (1) and (2) [11], [12]:

$$M^{2+} + 2(OH)^{-} \leftrightarrow M(OH)_2 \downarrow \quad (1)$$

$$R\text{-}COOH + Pb^{2+} \rightarrow R\text{-}COOPb^{2+} + H^{+} \quad (2)$$

The present study proposed the synthesis of a new hybrid, kenaf-chitosan-alginate (KNF-CHT-ALG) hydrogel composite beads and demonstrated the physical and chemical properties of the composite adsorbent. First, to identify the adsorbent with the most potential, two types of KNF samples were taken, the core and the fibre. Then, the composites were characterised using field emission scanning electron microscopy (FESEM), thermogravimetric analysis (TGA) and Fourier-transform infrared (FTIR) spectroscopy. The FESEM and TGA analyses were performed to assess the surface morphology and thermal properties of the proposed composites [13], [14]. The FTIR spectroscopy analysis illustrated the chemical properties of the proposed composites, enabling the identification of the functional groups present in the composites.

Batch mode sorption experiments with different parameters, including pH and contact time, were conducted

Manuscript received September 10, 2021; revised November 24, 2021. This work was supported under Fundamental Research Grant Scheme FRGS/1/2019/TK10/UITM/02/7.

N. A. S. Anuar, S. Abdul-Talib, S. Abdullah, J. Jaafar, and N. F. Lokman are with the School of Civil Engineering, College of Engineering, Universiti Teknologi MARA (UiTM), 40450 Shah Alam, Malaysia (e-mail: ainshafiqah_anuar@yahoo.com.my, ecsuhaimi@uitm.edu.my, sharifah.abdullah@uitm.edu.my, jurina@uitm.edu.my, nurul_fariha@uitm.edu.my).

T. Chia-Chay is with the Environmental Technology Program, Faculty of Applied Sciences, Universiti Teknologi MARA (UiTM), 40450 Shah Alam, Malaysia (e-mail: taychiay@uitm.edu.my).

S. Abdul-Talib, T. Chia-Chay, and N. F. Lokman are also with the MyBioREC, School of Civil Engineering, College of Engineering, Universiti Teknologi MARA (UiTM), 40450 Shah Alam, Malaysia.

doi: 10.18178/ijesd.2022.13.3.1375

to determine the removal of Pb (II) ions using the KNF-CHT-ALG beads as the sorbent. The removal percentage was verified through the inductively coupled plasma (ICP) analysis. Additionally, the adsorption kinetics of the synthesised adsorbents were determined using the fitted models of pseudo-first and pseudo-second orders.

II. Materials and Methods

A. Study Site and Sampling

Raw KNF samples were obtained from the Raw Material Collecting Centre (RMCC) owned by Lembaga Kenaf dan Tembakau Negara (LKTN) in Cherating, Kuantan, Pahang. Raw KNF samples were collected from the site and transported to the MyBioREC laboratory at the School of Civil Engineering, UiTM, Shah Alam.

B. Materials

The KNF core and fibre samples were cut. A sander machine was employed to turn the cut samples to powder. Lead(II) nitrate ($Pb(NO_3)_2$) purchased from R&M Chemicals was used to prepare Pb (II) ions solution in the desired concentration. Calcium chloride salts ($CaCl_2$) was also purchased from R&M Chemicals. Sodium alginate (ALG) and CHT powder purchased from Sigma Aldrich, Germany, were used to produce the adsorbents.

C. Preparation of the KNF Core and Fibre Samples

The collected raw KNF samples were cut into small chunks, around 30 cm each, and kept in a water basin for about 17 days. Fig. 1 displays the water retting process employed to ease the separation of the KNF fibre from its core. Subsequently, the samples were grounded, sieved and kept in air-tight plastic bags (Fig. 2). Finally, FESEM and TGA were employed to characterise the samples physically, while FTIR was utilised for chemical characterisation.

Fig. 1. The water retting process.

Fig. 2. The kenaf core and fibre samples powder after being sieved.

D. Characterisation of the KNF Core and Fibre Samples

Fig. 3 demonstrates the equipment utilised in the characterisation analyses of the proposed composites. The surface morphologies of the KNF core and fibre were observed using the FESEM Zeiss MERLIN at an accelerating voltage of 3.0 kV. The FESEM equipment was located at the Research Instrumental Management (RIM), Universiti Kebangsaan Malaysia (UKM). The FESEM analysis offered physical information at magnifications of 10× to 300000×, with nearly infinite depth of view. Compared to the traditional scanning electron microscopy (SEM), FESEM produced simpler and less electrostatically distorted images.

The thermal properties of the KNF core and fibre were investigated using the TGA analysis. The equipment employed was the Mettler-Toledo TGA/DSC Model in Instrumental Lab 2, School of Chemical Engineering, UiTM. The test was conducted in a nitrogen atmosphere with a 50 mL/min flow rate at 30 ℃ to 900 ℃ and a heating rate of 10 ℃/min. This technique offered easy operation with a small sample (1–20 mg).

The functional groups in the KNF core and fibre were subjected to FTIR analysis using a Spectrum One FTIR Spectrometer. The equipment used was also in Instrumental Lab 2, School of Chemical Engineering, UiTM. FTIR spectroscopy analysis is one of the most important analytical techniques available to investigate the chemical properties of various substrates. One of the main advantages of the approach is that various types of samples could be examined, including liquids, solutions, pastes, powders, films, fibres, and gases.

Fig. 3. The equipment used for characterisation analyses of FESEM (a) TGA (b) and FTIR (c).

E. Preparation of $Pb(NO_3)_2$ Solutions

The desired Pb(II) ions solution were obtained by dissolving 0.8 g of $Pb(NO_3)_2$ salts into 1 L conical flasks.

F. Preparation of the KNF-CHT-ALG Beads

The KNF-CHT-ALG beads were prepared by dissolving alginate (ALG) in ultrapure water (UPW) at 100 ℃ with magnetic stirring of 900–1200 revolutions per minute (rpm) for five minutes. The CHT powder was added to the solution and dissolved with 1% acetic acid. Next, the KNF core powder was added and stirred homogeneously. The blended solution then was dripped into 100 mL of calcium chloride to form smooth magnetic KNF-CHT-ALG beads. Finally, the beads were rinsed three times with UPW and dried at 60 ℃ for three hours.

G. Characterisation of the KNF-CHT-ALG Beads

The FESEM+EDX and FTIR equipment mentioned in Sect. D were employed to characterise the KNF-CHT-ALG beads.

H. Sorption Studies

The removal of Pb(II) ions by the KNF-CHT-ALG beads was studied using a batch sorption experiment conducted in 250 mL glass flasks. First, 0.5 g of adsorbent was added to the flask containing 50 mL of Pb(II) ions solution (a concentration of 50 mg/L). Then, the solution was shaken in an incubator shaker at 125 rpm for 60 minutes. Subsequently, the beads were filtered from the solution. The residual concentration of Pb(II) ions in the solution was analysed through ICP analysis. Finally, the adsorption percentage was calculated using the following equation [1]:

$$\text{Percentage of adsorption } (\%R) = (C_0 - C_t)/C_0 \times 100 \quad (3)$$

where C_0 is the Pb (II) ions concentration before adsorption (mg/l) and C_t is the Pb (II) ions concentration after adsorption (mg/l).

1) The effects of pH

The pH was maintained between 2.0 to 7.0 with aqueous 0.1 M nitric acid (HNO_3) and 0.1 M sodium hydroxide (NaOH). Simultaneously, the contact time, adsorbent dosage, and Pb (II) ions solution concentration were fixed at 60 minutes, 0.5 g, and 50 mg/L. Subsequently, the controlled parameters of the effects of pH were determined.

2) The effects of contact time

Approximately 0.5 g of the KNF-CHT-ALG adsorbent beads was mixed with 50 mL of Pb (II) solutions in a 250 mL conical flask at 50 mg/L. The solution was shaken for 5–60 minutes using a Thoth 6430 shaker model at 125 rpm. The final concentration of the Pb (II) ions was determined using an inductively coupled plasma optical emission spectrometer (ICP-OES).

I. Adsorption Kinetics

Pb (II) ions adsorption kinetics investigation was based on the pseudo-first and pseudo-second orders kinetic models. The pseudo-first and pseudo-second orders equations are defined by linear equations (4) and (5).

$$\log (q_e - q_t) = \log (q_e) - (k_1/2.303)t \quad (4)$$

$$t/q_t = 1/k_2 q_e^2 + t/q_e \quad (5)$$

where q_t (mg/g) is the amount of Pb (II) ions adsorbed at time t, and k_1 is the rate constant of adsorption (1/min). k_1 and q_e were be obtained from the intercept and slope of the linear graph of log $(q_e - q_t)$ versus time, t. In the pseudo-second order kinetic model, k_2 denotes the pseudo-second order rate constant (mg/g/min), and q_e is the amount of Pb (II) ions adsorbed at equilibrium. The linear plot of t/q_t versus time, t, was utilised to determine k_2 and q_e values, respectively.

III. Results and Discussion

A. Surface Morphology of the KNF Core and Fibre Samples

The FESEM micrographs that displayed the morphology of KNF core and fibre are shown in Fig. 4(a), (b), respectively. At 500× magnification, the KNF core exhibited a higher number of micropores compared to the KNF fibre. The findings were consistent with previous reports [15], [16], which reported that pore development increased the surface area, and the pore volume promoted the diffusion of heavy metal molecules into the pores.

According to [17], the surfaces of raw KNF are often rough. The same observation was reported by [18], which found that the KNF core exhibited better adhesion properties for the adsorption process when the surfaces were rougher. Comparably, the KNF core in this study provided preferable conditions that would improve the adsorption of heavy metals compared to the KNF fibre.

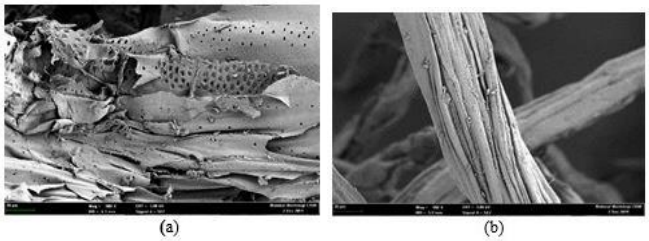

Fig. 4. FESEM images at 500× magnification and an accelerating voltage of 3.0 kV of KNF core (a) and fibre (b) samples.

B. Thermal Study of the KNF Core and Fibre Samples

Fig. 5 depicts the TGA thermograms, demonstrating the thermal decomposition behaviour of the KNF core and fibre samples. The KNF fibre thermally decomposed earlier compared to the KNF core. The phenomenon was caused by higher moisture absorption due to the presence of hemicelluloses. The percentage of weight reduction at 400 °C displayed the amount of residue left after the degradation of the composites.

The KNF fibre contained less residue compared to the KNF core due to the removal of lignin through alkalisation. Lignin in KNF is the primary cause for charring, contributing to higher char production in KNF fibre [19]. The charring produced by the degradation of the KNF fibre might improve the thermal resistance of its composites. Resultantly, the KNF fibre was more thermally resistant. However, the KNF fibre samples were less effective in trapping heavy metals because of their higher lignocellulosic components degradation, which led to the smoother surface of its composites [20].

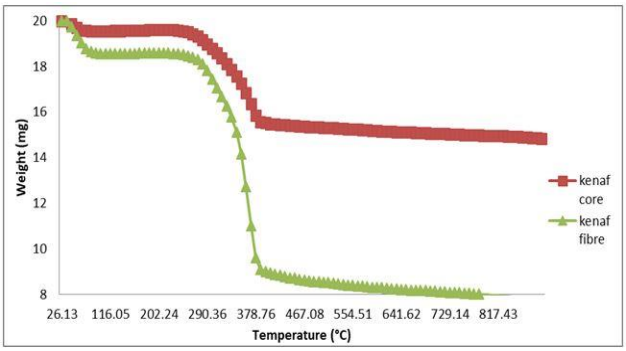

Fig. 5. TGA curves of the KNF core and fibre samples at a flow rate of 50 mL/min, the temperature of 30 °C to 900 °C, and a heating rate of 10 °C/min.

Table I shows the thermal decomposition temperature range and residual mass percentage after the KNF core and fibre samples underwent TGA. Based on the table, the KNF

core and fibre could hold a maximum heating temperature of 595 ℃ and 469 ℃, respectively. The maximum decomposition temperature for the KNF core was consistent with a previous report [21], which found that the maximum decomposition temperature of a KNF core was approximately 598 ℃.

In general, KNF plants consist of lignocellulosic components that mechanically support the plant, strengthen the plant, and help control biodegradation, thermal degradation, and moisture adsorption. An investigation reported that the mass of lignocellulosic components such as lignin, cellulose, and hemicellulose continued to decompose as temperature increased [22]. In this study, the initial weight for both samples were 20 mg. The KNF core exhibited a higher residue at 75.91% (15.18 mg) compared to the fibre sample at 43.09% (8.62 mg) due to a higher percentage of lignin content. The observation confirmed the results by [23], [24], in which a higher lignin content at 25.21% in the KNF core exhibited a higher residue percentage than the KNF fibre at 2.8% lignin content.

The weight decomposition displayed by the KNF core (24.09%) was lower than the KNF fibre (56.91%), indicating the degradation of lignocellulosic components in the core samples was much lower. The study by [22] highlighted that a higher percentage of weight reduction was primarily due to the increased degradation of the lignocellulosic components, promoting smoother and cleaner surfaces of KNF composites. Therefore, the KNF core was coarser and more irregular [25] than the KNF fibre, which could potentially assist the adsorption process of metal ions.

TABLE I: TGA RESULTS OF THE KNF CORE AND FIBRE SAMPLES

Sample	Decomposition temperature range (°C)	Maximum decomposition	
		Residue (%)	Weight loss (%)
Kenaf core	202 - 595	75.91	24.09
Kenaf fibre	227 - 469	43.09	56.91

C. Functional Groups Spectra of the KNF Core and Fibre Samples

The FTIR spectra of the KNF core and fibre samples are shown in Fig. 6(a), (b), respectively. Both the KNF core and fibre exhibited almost similar peaks. A wideband was observed at around 3300 cm^{-1} (peak I), confirming the presence of free hydroxyl (OH) groups imposing the functions of OH and carboxyl (COOH). Peak III band exhibited at around 1000 cm^{-1} corresponded to C-OH groups [26], [27]. Meanwhile, peak II at 1734 cm^{-1} attributed to the presence of –C=O, confirming the existence of carbonyl in the carboxyl group (-COOH) [28].

Both the KNF core and fibre samples confirmed the presence of functional groups and displayed potential in promoting the binding of metal ions. However, the KNF core was expected to demonstrate a better surface as its peaks I and III were more intense compared to the bands obtained from the KNF fibre samples. Therefore, only the KNF core was utilised to produce the KNF-CHT-ALG beads.

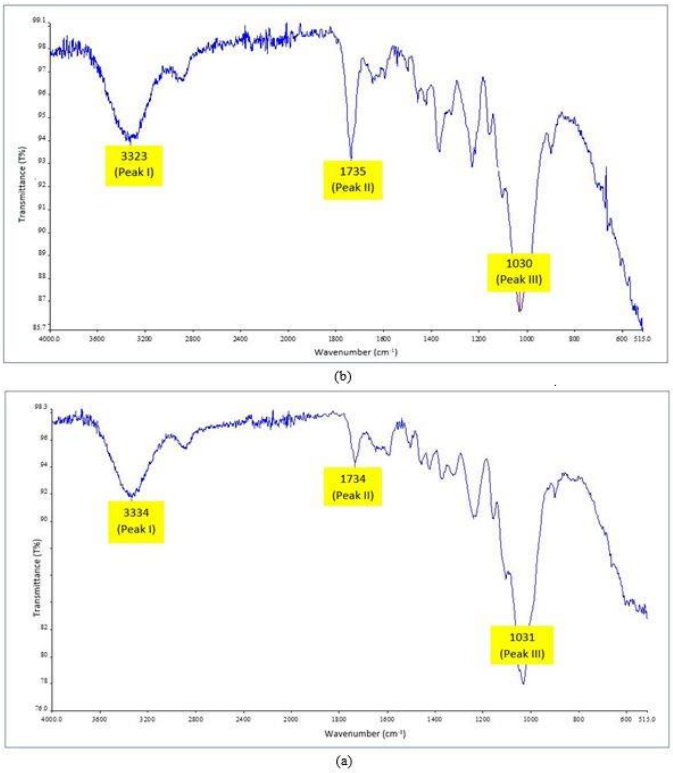

Fig. 6. FTIR spectra of the KNF core (a) and fibre (b) samples within the 515–4000 cm^{-1} range.

D. Surface Morphology of the KNF-CHT-ALG Beads before and after Adsorption of Pb (II) Ions

The surface morphology of the KNF-CHT-ALG beads before and after adsorption of Pb (II) ions are depicted in Fig. 7. The KNF-CHT-ALG beads, shown in Fig. 7(a), displayed rougher surfaces, indicating the presence of agglutinative flakes of fibrous cellulose materials that increased the adsorption rate of Pb (II) ions. Meanwhile, the image of the KNF-CHT-ALG beads after Pb (II) ions adsorption displayed in Fig. 7(b) were smoother and denser due to the formation of Pb (II) ions layer over the surface of the beads [29]. The observations were later confirmed with the EDX elemental spectra of the chemical composition of the beads.

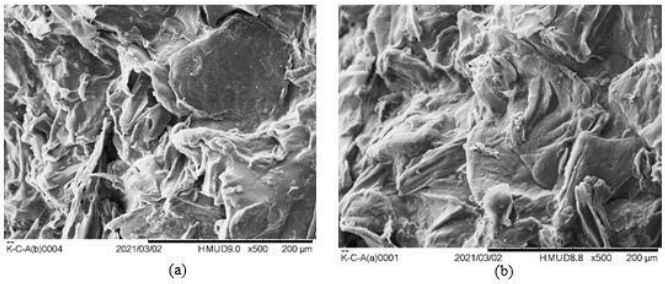

Fig. 7. FESEM images at 500× magnification and an accelerating voltage of 3.0 kV of the KNF-CHT-ALG before (a) and after (b) adsorption of Pb (II) ions.

Based on the EDX analysis illustrated in Fig. 8, the KNF-CHT-ALG beads before Pb (II) ions adsorption represented carbon, oxygen, calcium, and zirconium elements. Moreover, Pb peaks were detected on the surfaces of the beads after the adsorption of Pb (II) ions, confirming that the Pb (II) ions were adsorbed onto the KNF-CHT-ALG beads.

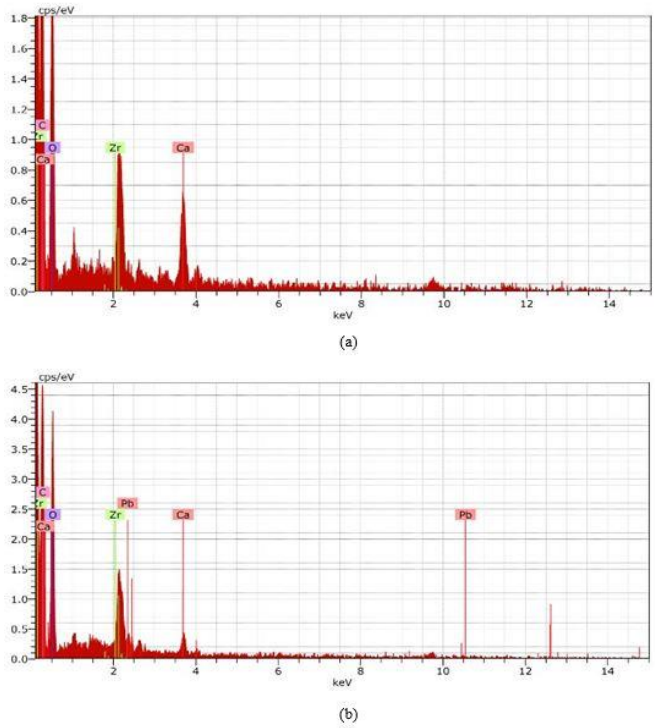

Fig. 8. The EDX spectra of the KNF-CHT-ALG beads before (a) and after (b) adsorption of Pb (II) ions.

E. Functional Groups Spectra of the KNF-CHT-ALG Beads

FTIR analysis was utilised to investigate further the functional groups present in the KNF-CHT-ALG beads to confirm the adsorption of Pb (II) ions. The results are displayed in Fig. 9. A wideband was observed within the 3200–3300 cm^{-1} range, confirming the presence of free OH groups imposing the OH functions in the beads [28]. The FTIR spectrum at around 1590 cm^{-1} might be due to the immobilisation of –C=O groups onto the cellulose groups of the KNF powder [10]. The band perceived within the 1416–1418 cm^{-1} region represented COO^- and C-O stretching, while the band within the 1008–1028 cm^{-1} range demonstrated the stretching vibration of ALG and CHT polymer [30]. The peak at 1734 cm^{-1} of the KNF-CHT-ALG beads confirmed the existence of the –C=O group in the -COOH group [28]. On the other hand, the peak at the 1244 cm^{-1} region corresponded to the C-O-C stretching vibration [10]. Overall, the KNF-CHT-ALG beads exhibited numerous functional groups, as illustrated by the FTIR spectra, confirming Pb (II) ions binding capabilities.

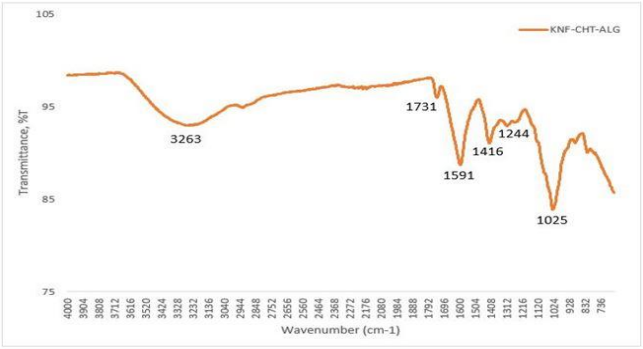

Fig. 9. FTIR spectra of the KNF-CHT-ALG beads within the 700–4000 cm^{-1} scanning range.

F. Heavy Metals Adsorption

The KNF-CHT-ALG beads that were analysed using the FESEM and the FTIR were initially tested for adsorption of Pb (II) ions. Table II illustrates several studies conducted on green KNF-based adsorbents in capturing heavy metals in wastewater. An investigation reported that the KNF fibre functionalised with phosphoric acid adsorped up to 88.2% of copper ions from electroplating wastewater [10]. In another study [31], the adsorption potential of a low-cost adsorbent Hibiscus Cannabicus KNF fibre investigated for Cr(VI) adsorption from water demonstrated a maximum Cr(VI) removal of 73%. Zinc chloride ($ZnCl_2$), used as a carbonising promoter for KNF core in treating heavy metal contamination, removed up to 91.2% manganese ions [32].

An investigation found that surface-modified CHT beads were more efficient in the adsorption of lead [29]. Based on the results, the current study proposed the synthesis of KNF-CHT-ALG beads, which exhibited 95% adsorption of Pb (II) ions upon further investigation. Additionally, the KNF core increased the adsorption binding capacity of the beads towards the Pb (II) ions.

TABLE II: PERCENTAGES OF HEAVY METALS REMOVAL BY GREEN MATERIAL-BASED ADSORBENTS

Adsorbents	Heavy metals	Percentage removal	References
Phosphoric acid modified kenaf fibre (K-PA)	Copper(II)	88.2%	[10]
Hibiscus Cannabicus kenaf fibre	Chromium(VI)	73.0%	[31]
$ZnCl_2$ carbonized kenaf core	Manganese(II)	91.2%	[32]
KNF-CHT-ALG	Lead(II)	95.0%	This study

G. Batch Adsorption Studies

1) The effects of pH

The pH of solutions is a critical parameter that affects the metal binding process and the availability of functional groups on the surface of adsorbents. The pH applied in the current investigation was within the 2–7 range. The effects of pH on the adsorption of metal ions by the KNF-CHT-ALG beads are depicted in Fig. 10. Based on the graph, the higher the pH, the higher the removal percentage. The maximum removal was at 96%, which was at pH 5. The findings were supported by a previous report [29], which demonstrated that at a lower pH, the positively-charged Pb (II) ions competed with the hydroxonium ions (H_3O^+), inducing a lower capture of the heavy metal ions. According to the same report, solutions at a higher pH improved the adsorption of Pb (II) ions. Solutions with a higher pH consist of an excess of hydroxyl ions (OH^-).

The beads were damaged and swollen at pH 2, while at pH above 5, a cloudy solution formed when Pb (II) ions were precipitated as lead hydroxide ($Pb(OH)_2$) (Fig. 11). The optimum pH observed was in agreement with a previous study [29], where the CHT beads surface modified with an anionic surfactant, sodium dodecyl sulfate (SDS), effectively removed up to 83.69% Pb (II) ions at pH 5. Additionally, another experiment [15] reported a higher percentage of removal that resulted from a pH close to neutral.

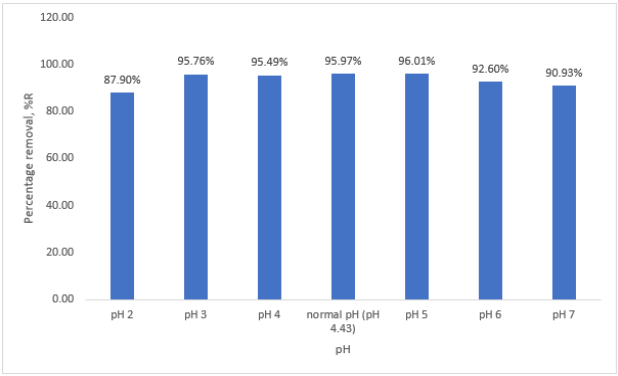

Fig. 10. The percentages of Pb (II) ions removal for adsorbent dosage of 0.5 g, 50 mg/L of Pb (II) ions concentration, and 60 min of contact time at pH 2–7.

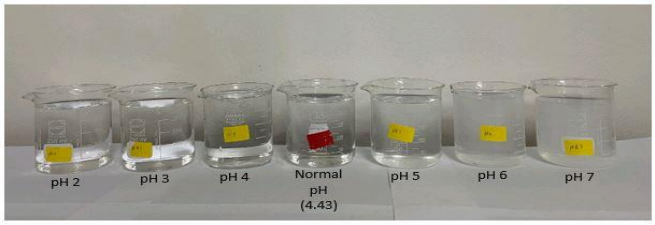

Fig. 11. The colour of Pb (II) solutions at pH 2–7.

2) *The effects of contact time*

The effects of contact time on Pb (II) ions adsorption by the KNF-CHT-ALG beads from an aqueous solution was investigated at different contact times within the range of 5–60 min. The concentration of Pb (II) ions used was 50 mg/L at an adsorbent weight of 0.5 g, and the pH of the solution was at the pH of 4.43 to reach maximum heavy metals extraction.

Fig. 12 displays the effect of contact time on Pb (II) ions removal over time. The rapid uptake of Pb (II) ions in the first 5 min were observed due to the high availability of vacant adsorption sites on the surface of the adsorbents followed by slow increments of removal after 40 min. The observations were due to increased repulsive forces of the adsorbed ions, making the remaining sites more difficult to access [33]. The optimal percentage of removal was reached at 60 min at 94%.

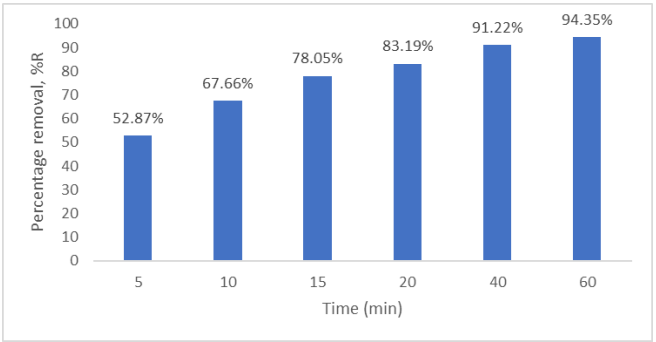

Fig. 12. The percentages of Pb (II) ions removal for adsorbent dosage of 0.5 g, 50 mg/L of Pb (II) ions concentration, and pH 4.43 at 5–60 min of contact time.

H. *Adsorption Kinetics*

The kinetic studies of Pb(II) ions adsorption on the KNF-CHT-ALG beads were carried out at 5, 10, 15, 20, 40, and 60 minutes using the pseudo-first order and pseudo-second order kinetic models. The adsorption was verified based on the highest value of regression coefficients (R^2) and the difference of the uptake capacity of calculated (q_e cal) and experimental (q_e exp) data [10]. Fig. 13(a), (b) illustrate the findings for both the pseudo-first and pseudo-second orders.

Fig. 13(a) plots the log ($q_e - q_t$) versus time, t, graph, which was inversely proportional for the pseudo-first order. Based on the figure, the R^2 value was 0.9766. On the other hand, Fig. 13(b) depicts the graph of t/q_t versus time, t, which was linear for the pseudo-second order. According to the results, the R^2 value was 0.9999, which was significantly higher than the pseudo-first order.

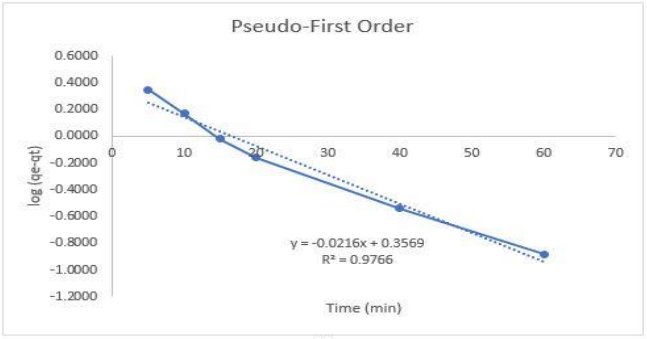

(a)

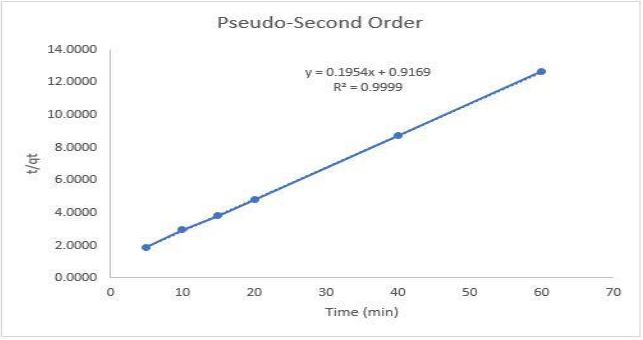

(b)

Fig. 13. Kinetic plots for adsorption of Pb (II) ions onto KNF-CHT-ALG beads for the pseudo-first order (a) and pseudo-second order (b) of adsorbent dosage of 0.5 g, 50 mg/L of Pb (II) ions concentration, and 50 mL of Pb(II) ions.

Table III shows the rate constants of the pseudo-first and pseudo-second orders calculated from the equation in Sect. I. The R^2 values obtained for the pseudo-first order was 0.9766 and considered satisfactory. Nonetheless, a significant difference was observed between the experimental value of q_e (4.8729 mg/g) and the calculated q_e (2.275 mg/g) obtained from the linear plot. The results suggested that the pseudo-first order model did not sufficiently support the adsorption data. On the other hand, the R^2 obtained for the pseudo-second order was 0.9999, which was higher than the pseudo-first order model and the nearness of experimental q_e (4.8729 mg/g) and calculated q_e (5.118 mg/g) proved that this model was well fitted for explaining the Pb (II) ions adsorption onto KNF-CHT-ALG beads. The observations also aligned with the research by [10] and [34].

TABLE III: RATE CONSTANTS FOR THE KINETIC MODELS OF PB (II) IONS ADSORPTION

Metal ion	q_e exp (mg/g)	Pseudo-first order			Pseudo-second order		
		k_1(1/min)	q_e cal (mg/g)	R^2	k_2(mg/g/min)	q_e cal (mg/g)	R^2
Pb(II)	4.8729	0.0497	2.275	0.9766	0.0416	5.118	0.9999

IV. Conclusion

The current study investigated the physical and chemical properties of the KNF core and fibre through FESEM, TGA, and FTIR analyses. According to the FESEM micrographs, the KNF core exhibited more micropores and surface roughness than the KNF fibre. Therefore, the KNF core offered more adhesion surfaces for the adsorption of metal ions, including Pb (II) ions. Furthermore, as shown in the TGA analysis, the KNF core exhibited higher surface roughness due to its high residue of up to 75.91% at maximum decomposition temperature. In FTIR spectra analysis, both the KNF core and fibre samples exhibited similar functional groups (OH, C-OH, and –C=O), suitable for heavy metals adsorption. Interestingly, the KNF core consisted of a better surface as there were two peaks with high intensity compared to the KNF fibre.

The KNF-CHT-ALG beads that utilised the KNF core were successfully synthesised. The KNF-CHT-ALG beads exhibited numerous suitable functional groups and illustrated a porous microstructure with sufficient surface area to provide more reaction sites for Pb(II) ions for up to 95% adsorption. The adsorption kinetics was also in good agreement with the pseudo-second order model with an R^2 value of 0.9999. The findings demonstrated that the KNF-CHT-ALG beads are adsorbents that could potentially be utilised for future adsorption of other metal ions.

Conflict of Interest

On behalf of all the authors involved, the corresponding author wishes to state that there is no conflict of interest.

Author Contributions

N. A. S. Anuar conducted the research. N. A. S. Anuar, N. F. Lokman and T. Chia-Chay analysed the research data, and finally, all authors contributed ideas for the paper writing and approved the final version of this manuscript.

Acknowledgment

This study was financially supported by the Fundamental Research Grant Scheme (FRGS) (Grant number: FRGS/1/2019/TK10/UITM/02/7). The authors are also infinitely grateful to the Lembaga Kenaf Dan Tembakau Negara (LKTN) Pahang, MyBioREC Laboratory, School of Civil Engineering, College of Engineering, Universiti Teknologi MARA, Shah Alam, Selangor, Instrumental Lab 2 Laboratory, School of Chemical Engineering, Universiti Teknologi MARA, Shah Alam, Selangor, and the Centre for Research and Instrumentation Management (CRIM), Universiti Kebangsaan Malaysia, Bangi, for the permission to utilise their facilities.

References

[1] S. Biswas, R. K. Prabhu, S. Vijayalakshmi, and R. C. Panigrahy, "Concentration of heavy metals in the food chain components of the nearshore coastal waters of Kalpakkam, southeast coast of India," *Food Control*, vol. 72, pp. 232-243, 2017.

[2] M. F. Ahmed, M. Mokhtar, L. Alam, C. A. R. Mohamed, and G. C. Ta, "Investigating the status of cadmium, chromium and lead in the drinking water supply chain to ensure drinking water quality in Malaysia," *Water*, vol. 12, pp. 1-26, 2020.

[3] S. Cheng, Y. Liu, B. Xing, X. Qin, and C. Zhang, "Lead and cadmium clean removal from wastewater by sustainable biochar derived from poplar saw dust," *J. Clean. Prod*, vol. 314, pp. 128074, 2021.

[4] S. Mandal, J. Calderon, S. B. Marpu, M. A. Omary, and S. Q. Shi, "Mesoporous activated carbon as a green adsorbent for the removal of heavy metals and Congo red : Characterization , adsorption kinetics , and isotherm studies," *J. Contam. Hydrol*, vol. 243, pp. 103869, 2021.

[5] G. Fadillah, E. N. K. Putri, S. Febrianastuti, E. V. Maylinda, and C. Purnawan, "Adsorption of Fe ions from aqueous solution using α -keratin-coated alginate biosorbent," *Int. J. Environ. Sci. Dev*, vol. 9, pp. 82–85, 2018.

[6] A. Lamplugh, M. Harries, A. Nguyen, and L. D. Montoya, "VOC emissions from nail salon products and their effective removal using affordable adsorbents and synthetic jets," *Build Environ*, vol. 168, pp. 106499, 2020.

[7] U. Rakchaiyawan, Y. Kulratkitiwong, and K. Piyamongkala, "Kinetics adsorption of silver ion by blend chitosan-polyvinyl alcohol resin," *Int. J. Environ. Sci. Dev*, vol. 6, pp. 6–10, 2015.

[8] M. Pulat, "The preparation of gelatin coated sodium alginate hydrogels," *The Eurasia Proceedings of Science, Technology, Engineering & Mathematics (EPSTEM)*, pp. 149–155, vol. 4, 2018.

[9] U. Berardi and G. Iannace, "Acoustic characterization of natural fibers for sound absorption applications," *Build Environ*, vol. 94, pp. 840–852, 2015.

[10] M. Raznisya, N. Azah, A. Zaharin, H. Mohmad, J. Haron, N. Azowa, and I. Syazana, "Phosphoric acid modified kenaf fiber (K-PA) as green adsorbent for the removal of copper (II) ions towards industrial waste water effluents," *React Funct Polym*, vol. 147, pp. 104466, 2020.

[11] M. J. Baniamerian, S. E. Moradi, A. Noori, and H. Salahi, "The effect of surface modification on heavy metal ion removal from water by carbon nanoporous adsorbent," *Appl. Surf. Sci*, vol. *256*, pp. 1347–1354, 2009.

[12] M. A. Barakat,"New trends in removing heavy metals from industrial wastewater," *Arab. J. Chem*, vol. *4*, pp. 361–377, 2011.

[13] J. Sai Revanth, V. Sai Madhav, Y. Kalyan Sai, D. Vineeth Krishna, K. Srividya, and C. H. Mohan Sumanth, "TGA and DSC analysis of vinyl ester reinforced by Vetiveria zizanioides, jute and glass fiber," *Mater. Today*, vol. 26, pp. 460-465, 2020.

[14] V. A. Baki, S. Nayır, Ş. Erdoğdu *et al*., "Determination of the pozzolanic activities of trachyte and rhyolite and comparison of the test methods implemented," *Int J Civ Eng*, vol. 18, pp. 1053–1066, 2020.

[15] R. Shamsudin, H. Abdullah, and A. Kamari, "Application of kenaf bast fiber to adsorb Cu (II), Pb (II) and Zn (II) in aqueous solution: Single- and multi-metal systems," *Int. J. Environ. Sci. Dev*, vol. 7, 2016.

[16] M. S. Shamsuddin, N. R. N. Yusoff, and M. A. Sulaiman, "Synthesis and characterization of activated carbon produced from kenaf core fiber using H3PO4 activation," *Procedia Chem*, vol. 19, pp. 558–565, 2016.

[17] N. Afiqah, M. Radzuan, D. Tholibon, A. B. Sulong, N. Muhamad, C. Hassan, and C. Haron, "New processing technique for biodegradable kenaf composites: A simple alternative to commercial automotive parts," *Compos. B. Eng*, vol. 184, pp. 107644, 2020.

[18] A. M. Adole, J. M. Yatim, S. A. Ramli, A. Othman, and N. A. Mizal, "Kenaf fibre and its bio-based composites: A conspectus," *Pertanika J. Sci. Technol*, vol. 27, pp. 297–329, 2019.

[19] H. A. Saffian, M. A. Talib, S. H. Lee, P. M. Tahir, C. H. Lee, H. Ariffin and A. Z. M. Asa'ari, "Mechanical strength, thermal conductivity and electric breakdown of kenaf core fiber/lignin/polypropylene biocomposite," *Polymers*, vol. 12, pp. 1833, 2020.

[20] Z. N. Azwa and B. F. Yousif, "Characteristics of kenaf fibre / epoxy composites subjected to thermal degradation," *Polym. Degrad. Stab*, vol. 98, pp. 2752–2759, 2013.

[21] S. Abdullah and R. M. Tajuddin, *Thermal Gravimetric Analysis (Tga) of Kenaf Core and Its Cellulose for Membrane Fabrication*, 2015, pp. 667-677.

[22] M. Athmalingam and V. W. Vicki, "Investigation on thermal properties of kenaf fibre reinforced polyurethane bio-composites," *IOP Conference Series: Material Science and Engineering*, vol. 303, pp. 012011, 2017.

[23] S. Zakaria, R. Roslan, and C. Chia, "Characterization of residue from EFB and kenaf core fibres in the liquefaction process," *Sains Malays*, vol. 43, pp. 429-435, 2014.

[24] H. M. Akil, M. F. Omar, A. A. M. Mazuki, S. Safiee, Z. A. M. Ishak, and A. A. Bakar, "Kenaf fiber reinforced composites : A review," *Mater. Des*, vol. 32, pp. 4107–4121, 2011.

[25] Y. Song, W. Jiang, Y. Zhang, H. Ben, G. Han, and A. J. Ragauskas, "Isolation and characterization of cellulosic fibers from kenaf bast

using steam explosion and Fenton oxidation treatment," *Cellulose*, vol. 25, pp. 4979–4992, 2018.
[26] D. Tuerxun, T. Pulingam, N. I. Nordin, Y. W. Chen, J. Kamaldin, N. M. Julkapli, H. V. Lee, B. F. Leo, and M. R. Johan, "Synthesis, characterization and cytotoxicity studies of nanocrystalline cellulose from the production waste of rubber-wood and kenaf-bast fibers," *Eur. Polym. J*, vol. 116, pp. 352–360, 2019.
[27] A. A. S. Javid, P. Ghoddousi, M. Zareechian *et al*., "Effects of spraying various nanoparticles at early ages on improving surface characteristics of concrete pavements," *Int J Civ Eng*, vol. 17, pp. 1455–1468, 2019.
[28] G. Z. Kyzas, Z. Terzopoulou, V. Nikolaidis, E. Alexopoulou, and D. N. Bikiaris, "Low-cost hemp biomaterials for nickel ions removal from aqueous solutions," *J. Mol. Liq*, vol. 209, pp. 209–218, 2015.
[29] P. Pal and A. Pal, "Enhanced Pb2+ removal by anionic surfactant bilayer anchored on chitosan bead surface," *J. Mol. Liq*, vol. 248, pp. 713–724, 2017.
[30] P. Karthikeyan, H. A. T. Banu, and S. Meenakshi, "Synthesis and characterization of metal loaded chitosan-alginate biopolymeric hybrid beads for the efficient removal of phosphate and nitrate ions from aqueous solution," *Int. J. Biol. Macromol*, vol. 130, pp. 407–418, 2019.
[31] M. Omidvar, M. Pirsaheb, M. Vosoughi, R. Khosravi, B. Kakavandi, M. Reza, and A. Asadi, "Batch and column studies for the adsorption of chromium (VI) on low-cost Hibiscus Cannabinus kenaf, a green adsorbent," *J. Taiwan Inst. Chem. Eng*, vol. 68, pp. 80–89, 2016.
[32] M. R. Othman, H. M. Akil, and J. Kim, "Carbonaceous hibiscus cannabinus L. for treatment of oil- and metal-contaminated water," *Biochem. Eng. J*, vol. 41, pp. 171–174, 2008.
[33] A. A. Alghamdi, W. S. Saeed, A. Al-kahtani, F. A. Alharthi, and T. Aouak, "Efficient Adsorption of lead(II) from aqueous phase solutions using polypyrrole-based activated carbon," *Materials*, vol. 12, 2020.
[34] M. M. Kabir, S. S. P. Mouna, S. Akter, S. Khandaker, M. Didar-ul-Alam, N. M. Bahadur, M. Mohinuzzaman, M. A. Islam, and M. A. Shenashen, "Tea waste based natural adsorbent for toxic pollutant removal from waste samples," *J. Mol. Liq*, vol. 322, pp. 115012, 2021.

N. A. S. Anuar is currently a postgraduate student in master of science in civil engineering, School of Civil Engineering, College of Engineering, Universiti Teknologi MARA (UiTM). Her research interest focuses on kenaf-based sorbent materials.

S. Abdul-Talib is a professor at School of Civil Engineering, Universiti Teknologi MARA (UiTM). In 1996, he obtained his master of science in water and environmental management with distinction at University of Loughborough, UK and in 2002 he completed his Ph.D. in water and wastewater engineering at the Universiti Teknologi Malaysia (UTM). As a researcher he had acquired research grants totalling more than RM 2 million and had published and presented more than 200 papers. He had delivered more than 50 keynote and invited lectures.

T. Chia-Chay is an associate professor in environmental technology program, Faculty of Applied Sciences, Universiti Teknologi MARA (UiTM). She has published more than 30 peer-reviewed journals and is active in reviewing journals. She received the best paper award in International Conference on Advances in Civil and Environmental Engineering (2015) and a few innovation prizes. She also hosted DAAD RISE Worldwide Research Internship Program in 2015 and joined ASEA-UNINET International Community Outreach Program: Life below Water in 2019.

S. Abdullah is a senior lecturer at School of Civil Engineering, College of Civil Engineering, Universiti Teknologi MARA (UiTM). Her field of expertise are membrane technology, river engineering, mudball, wastewater quality improvement and organic material coagulation. She has 26 years of teaching experience in Civil Engineering subjects. Her current research is focusing on membrane technology, Kenaf materials and application of mudball as the bio-filtration.

J. Jaafar obtained her master's degree in water resources engineering and management from University of Stuttgart, Germany. Subsequently, she obtained a PhD in civil engineering (hydrodynamic and hydrology engineering) from Universiti Teknologi MARA (UiTM), Malaysia. She has been serving UiTM since January 2003 as a senior lecturer at the School of Civil Engineering. Her research interest includes hydrodynamic and hydrological modeling, water resources engineering and environmental engineering.

N. F. Lokman is a senior lecturer at School of Civil Engineering, Universiti Teknologi MARA (UiTM). In 2010, she earned her Master of Civil Engineering from UiTM. Her research work for master degree has been conducted at Nagaoka University of Technology, Japan. Her honors pHD from Universiti Kebangsaan Malaysia in year 2016 was about detection of Pb-metals in water using Surface Plasmon Resonance (SPR) sensors system. Currently, she is actively conducting research on Kenaf-sorb beads originating from kenaf core which is for adsorption of heavy metals in aqueous solution.